Nanoscale

Magnetic Control of Electrochemical Processes at Electrode Surface using Iron-rich Graphene Materials with Dual Functionality

Journal:	*Nanoscale*
Manuscript ID:	NR-ART-04-2014-001985
Article Type:	Paper
Date Submitted by the Author:	12-Apr-2014
Complete List of Authors:	Lim, Chee Shan; Nanyang Technological University, Chemistry and Biological Chemistry Ambrosi, Adriano; Nanyang Technological University, Chemistry and Biological Chemistry Sofer, Zdenek; Institute of Chemical Technology, Prague, Department of Inorganic Chemistry Pumera, Martin; Nanyang Technological University, Chemistry and Biological Chemistry

Journal Name

RSCPublishing

ARTICLE

Magnetic Control of Electrochemical Processes at Electrode Surface using Iron-rich Graphene Materials with Dual Functionality

Chee Shan Lim[a], Adriano Ambrosi[a], Zdenek Sofer[b] and Martin Pumera[a]

Cite this: DOI: 10.1039/x0xx00000x

Received ooth January 2012,
Accepted ooth January 2012

DOI: 10.1039/x0xx00000x

www.rsc.org/

Metal-doped graphene hybrid materials demonstrate promising capabilities in catalysis and various sensing applications. There also exists great interest for on-demand control of selectivity of many electrochemical processes. In this work, an iron-doped thermally-reduced graphene oxide (Fe-TRGO) were prepared and used to investigate the possibility of a reproducible, magnetically-controlled method to modulate electrochemical reactivities through a scalable method. We made use of the presence of both magnetic and electrocatalytic properties in the Fe-TRGOs to induce attraction and removal of the Fe-TRGO material onto and off the working electrode surfaces magnetically, thereby controlling the electrochemical oxidation and reduction processes. The outstanding electrochemical performance of the Fe-TRGO material was evident with enhanced current signals and lower peak potentials observed upon magnetic activation. Reversible and reproducible cycles of activation and deactivation were obtained as the peak heights and peak potentials remained relatively consistent with no apparent carryover between every step. Both components of Fe-TRGO play an electrocatalytic role in the electrochemical sensing. In the cases of oxygen reduction reaction and reduction of cumene hydroperoxide, the iron oxide plays the role of an electrocatalyst while the in the cases of ascorbic acid, the enhanced electroactivity originates from the high surface area of the graphene portion in the Fe-TRGO hybrid material. The feasibility of this magnetically-switchable method for on-demand sensing and energy production thus brings about potential developments for future electrochemical applications.

1. Introduction

Graphene is a one layer thick, two-dimensional material with a sp^2-bonded carbon network arranged in a honeycomb lattice.[1] Increasing emphasis has been re-placed on it among the electrochemistry community over the recent years owing to their exceptional electrochemical performance and one-of-a-kind characteristics, such as high surface area,[2] high electron mobility[3] and fast heterogeneous electron transfer rates.[4]

Despite so, the absence of defects and semiconducting band gap[5] on pristine graphene serve as drawbacks in electrochemical sensing. This led to a series of modifications explored and carried out on graphene to produce materials with more competitive properties and better electrochemical performances. Of which, chemically modified graphenes are a prominent group of graphene-related materials which can be synthesized *via* oxidation of graphite to graphite oxide, followed by a chemical, thermal or electrochemical reduction in general.2,6 Lately, another modification consisting of the addition of metal nanoparticles onto graphene, also known as metal doping, has been commonly used.[7,8] Doped graphenes have been known to possess the abilities to modify band gap[9,10] and control the semiconducting properties of graphene;5 graphene-metal hybrid systems have also become increasingly prominent in sensing and catalysis applications thus far.[11]

On top of band gap tuning, metal-doped graphenes have been widely exploited to realise a challenging objective of on-demand control of selectivity of electrochemical processes due to their dual properties, magnetic and electrocatalytic. On-demand sensing has become of paramount importance in sensing applications due to its convenience and effectiveness in the execution of electrochemical studies. Previous works which have successfully demonstrated on-demand electrochemical control and sensing include magneto-switchable control of electrochemical reactivity using carbon nanotubes (CNTs),[12] on-demand microsystem control using nanowires,[13] methanol oxidation carried out with controlled bimetallic nanoparticles[14] and magnetic control of electrochemical processes *via* nickel particles.[15] These findings have exemplified the advantage of

the combined properties in metal-doped graphenes in achieving improved sensing at ease and efficiency.

Despite so, limited studies have been done in the recent years to further explore this novel methodology. Here, we introduce a scalable methodology *via* a graphene-iron hybrid system, which aspires to be of considerable use to on-demand sensing and key electron-transfer reactions without the need for functionalised magnetic particles. An iron-doped thermally reduced graphene oxide (Fe-TRGO) has been prepared and used to study the electrocatalysis of three different molecules, ascorbic acid, potassium, cumene hydroperoxide and oxygen reduction reaction. Magnetically-controlled reversibility of the electrochemical processes in terms of surface reactivity and sensitivity are discussed and avowed in this work, as we also examine the feasibility of this system on oxygen reduction reaction (ORR), an imperative industrial process in particular.

2. Experimental

2.1 Materials

Sulphuric acid (98 %), sodium nitrate (>99.5 %), potassium permanganate (>99 %), hydrogen peroxide (30 %), iron(III) nitrate nonahydrate (>99 %) and barium nitrate (>99.5 %) were obtained from Lach-Ner, Czech Republic. Graphite microparticles (2-15 μm, 99.9995%) were obtained from Alfa Aesar, Germany. The gases were obtained from SIAD, Czech Republic (Nitrogen 99.9999 %, Hydrogen 99.9999 %). *N,N*-dimethylformamide (DMF), potassium phosphate monobasic, sodium phosphate dibasic, potassium chloride, sodium chloride, potassium hydroxide, ascorbic acid, cumene hydroperoxide were purchased from Sigma-Aldrich, Singapore. Three-E screen-printed electrodes (SPEs) of working diameter 3 mm were obtained from Zensor, Taiwan. Milli-Q water with a resistivity of 18.2 MΩcm was used throughout the experiments.

2.2 Apparatus

Scanning electron microscopy (SEM) images were obtained with a Jeol 7600F SEM (Jeol, Japan), which operates at 10 kV, and the backscattering image at 5 kV. Energy-dispersive X-ray spectroscopy (EDX) was documented on a Jeol 7600F (Jeol, Japan) at 15 kV. X-ray photo-electron spectroscopy (XPS) measurements were performed using a Phoibos 100 spectrometer and a monochromatic Mg X-ray radiation source (SPECS, Germany). Survey (wide scan) spectra and high-resolution spectra of C1s, O1s and Fe2p were taken for each sample. C/O ratios were determined from the survey spectra by using relative sensitivity factors. For SEM, SEM-EDX, and XPS measurements, sample preparation was done by coating a uniform layer of the materials investigated on a carbon conductive tape.

Cyclic voltammetry and linear sweep voltammetry were carried out with a μAutolab type III electrochemical analyser (Eco Chemie, The Netherlands) connected to a personal computer and controlled by NOVA 1.8 software. All voltammetry experiments were performed in a 5 mL electrochemical cell at room temperature using the three-electrode system present on the SPEs, with an Ag/AgCl reference electrode surface and a platinum counter electrode surface around the working electrode surface. All electrochemical potentials in this report are stated *vs.* the Ag/AgCl reference electrode.

2.3 Procedure

Graphite oxides were first synthesized using the Hummers method.[16] 5 g of graphite and 2.5 g of sodium nitrate were stirred with 115 mL of concentrated sulfuric acid. The mixture was then cooled on 0 °C. With vigorous stirring, 15 g of potassium permanganate was then added over a period of two hours. In the subsequent four hours, the reaction mixture was allowed to reach room temperature before being heated to 35 °C for 30 min. The reaction mixture was then poured into a flask containing 250 mL of deionized water and heated to 70 °C for 15 minutes. The mixture was then poured into 1 L of deionized water. The unreacted potassium permanganate and manganese dioxide were removed by the addition of 3 % hydrogen peroxide. The reaction mixture was then allowed to settle and decanted. The graphite oxide obtained was then purified by repeated centrifugation and re-dispersed in deionized water until a negative reaction on sulfate ion (with $Ba(NO_3)_2$) was achieved. Graphite oxide slurry was then dried in a vacuum oven at 50 °C for 48 h before use.

The Fe-TRGO was prepared by thermal exfoliation of Fe-doped graphene oxide in hydrogen atmosphere. 200 mg of graphite oxide was exfoliated in 50 ml water by ultrasonication (400 W, 120 minutes). The suspension containing 200 mg of graphene oxide were added to the solution containing $Fe(NO_3)_3.9H_2O$ in sufficient amount to make the Fe-doped graphene oxide. The reaction mixture was dried in vacuum oven (50 °C, 48 h). These iron-doped graphene oxides then underwent a heat treatment of 12 minutes at 1000 °C under pure H_2 atmosphere for exfoliation to occur, eventually forming respective Fe-TRGOs. 100 mg of graphene oxide was placed inside the quartz glass capsule connected to a magnetic manipulator and placed inside the horizontal quartz glass reactor. Before the insertion of the sample within the hot zone, the reactor was repeatedly evacuated and flushed with nitrogen. Subsequently, the nitrogen flow was switched to hydrogen and the sample was inserted in the hot zone of the reactor. The sample was maintained at 1000 °C for 12 minutes. A hydrogen flow at 1000 $mLmin^{-1}$ was used to remove the by-products from the exfoliation process. After the end of reaction procedure, the sample was removed from hot zone of the reactor and whole apparatus was flushed with nitrogen prior to opening.

The powdered Fe-TRGO was dispersed in DMF with a concentration of 1 mg mL^{-1} and ultrasonicated for 60 minutes to obtain a homogeneous suspension. 10 μL aliquot of the suspension was deposited onto the electrode surface and kept in

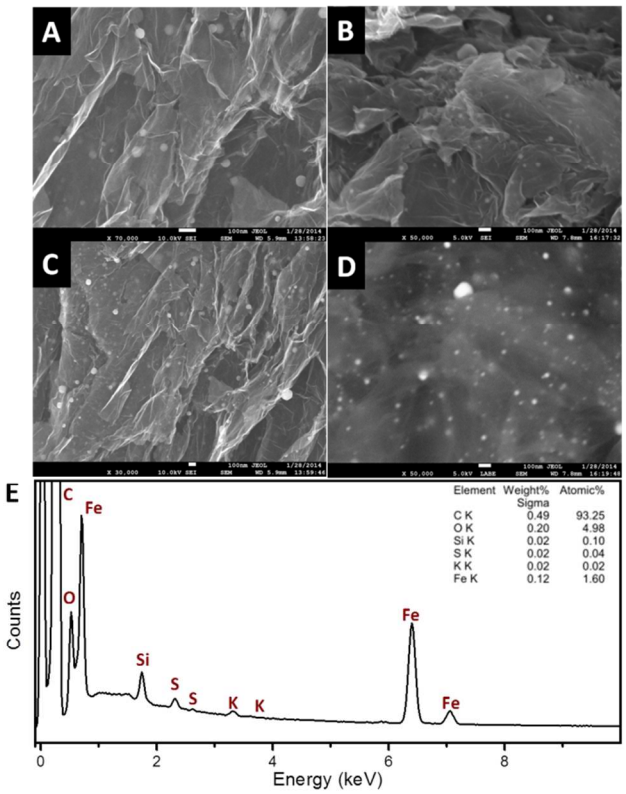

Figure 1. SEM images at magnifications of (A) 70,000 x, (B) 50,000 x, (C) 30,000 x and (D) backscatter image at 50,000 x, with scale bars of 100 nm for all images, together with (E) SEM/EDX spectra of the Fe-TRGO material.

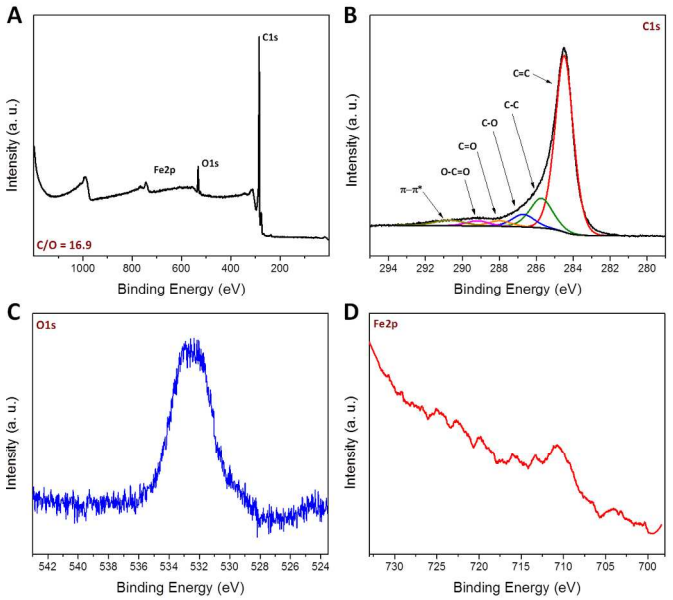

Figure 2. XPS high resolution spectra of (A) survey scans, (B) C1s, (C), O1s and (D) Fe2p for the Fe-TRGO material.

suspension form throughout measurements to ensure and maximise mobility of the iron-graphene material.

The reproducibility of the measurements was obtained over 3 experiments each time, using fresh electrode units. All voltammetry measurements were conducted in a 50 mM phosphate buffer solution of pH 7.2.

3. Results and Discussion

3.1 Characterisation

Prior to the demonstration of the magneto-switchable on-demand electrocatalytic effect of the Fe-doped graphene hybrid, characterisation of the Fe-TRGO material was performed *via* techniques such as scanning electron microscopy (SEM), energy-dispersive X-ray spectroscopy (EDX) and X-ray photoelectron spectroscopy (XPS).

The morphology of the Fe-TRGO material was investigated using the SEM technique. Figures 1A to 1C show the structure of the TRGO at different magnifications. Thin sheets of graphene oxides were observed, affirming that exfoliation from graphene oxide to TRGO has taken place. Small white agglomerates of iron are apparent in the SEM images as well, but more so in the backscatter image (D), indicating successful doping of the iron particles onto the TRGO.

Elemental analysis was also carried out using the SEM/EDX technique to identify the various elements and their atomic percentage ratios, as shown in image E and the inset. High levels of carbon and oxygen which correspond to the composition of graphene oxide were present in the material, comprising about 93 at% and 5 at% of the sample, respectively. The metal dopant, iron, made up about 1.60 at% of this material. Impurities such as silicon, sulfur and potassium were also present in the sample, despite in negligible amounts of less than 0.2 at% in total.

The surface composition of the material, including the types of elements present as well as their chemical environments was defined using XPS, a surface-sensitive technique with detection limits as low as 0.1 wt% of the sample.[17] The survey spectrum of the Fe-TRGO material shows rather prominent carbon and oxygen peaks, with relatively small iron peaks as shown in image A of Figure 2. This may be attributed to the insignificant amounts of iron present on the surfaces of the material, hence resulting in peaks which are not too evident. The carbon/oxygen (C/O) ratios of the material was also provided in the survey scan. The Fe-TRGO material has a C/O ratio of about 16.9, much larger than that of a normal GO material prepared by the Hummers method (~2.05).[18] This implies that a substantial amount of oxygen functionalities has been reduced *via* the thermal reduction method.

Figure 2B displays the high resolution carbon scan spectra, C1s, elaborating on the various types of chemical bonding present between the atoms. Evidently, there were significantly lower amounts of epoxy, carbonyl and carboxyl groups compared to alkyl and alkene groups. This observation further affirms the large extent of removal of the oxygen-containing

groups present in the inherent graphite oxide following thermal reduction.

As illustrated in Figure 2C, one slightly broad peak was observed in the high resolution core level spectrum of O1s, with a binding energy of around 531.5 to 533.0 eV. This peak corresponds to oxygen in organic C–O or C=O bonds, which coincides with the functionalities found earlier in the C1s spectra for TRGO. Possible overlapping might have occurred due to the close binding energies of the various bonds, thus giving a slightly broad peak instead.

However, the core level spectra of Fe 2p failed to produce very apparent peaks, as exhibited in Figure 2D. The only noticeable peak was seen at a binding energy of around 710.0 eV, corresponding to the Fe $2p_{3/2}$ spin pattern.

3.2 Magnetic Acitvation/Deactivation of Electrochemical Processes

A 3-electrode SPE was employed to carry out the electrochemical measurements, with an external magnet positioned underneath the electrode to manipulate the position of the Fe-TRGO materials as illustrated in Figure 3. The activation process was accomplished by placing the magnetic Fe-TRGO material onto the working electrode surface (Figure 3A), while deactivation was obtained by moving the magnet away from the electrode surface and remving the Fe-TRGO particles from the working electrode surface as a result (Figure 3B). Several on and off cycles can thus be generated reproducibly. The electrochemical performance of the magnetic Fe-TRGO material was investigated *via* cyclic voltammetry studies and using ascorbic acid and cumene hydroperoxide as redox probes. Linear sweep voltammetry studies were also carried out to evaluate the catalytic properties of the materials towards the oxygen reduction reaction (ORR) in alkaline medium. The Fe-TRGO material plays various electrocatalytic roles in different probes. Iron oxides have been known electrocatalysts for electrochemical reduction of ORR and cumene hydroperoxide[19] (whilst graphene plays only a conducting support role[20]) while in the case of ascorbic acid, the graphene portion of Fe-TRGO hybrid becomes the determining factor in generating enhanced currents due to its large surface area.

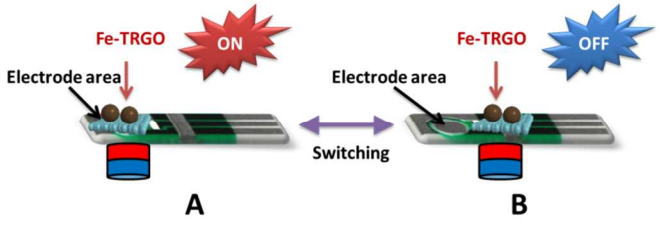

Figure 3. Experimental setup for (A) activation and (B) deactivation of electrochemical process.

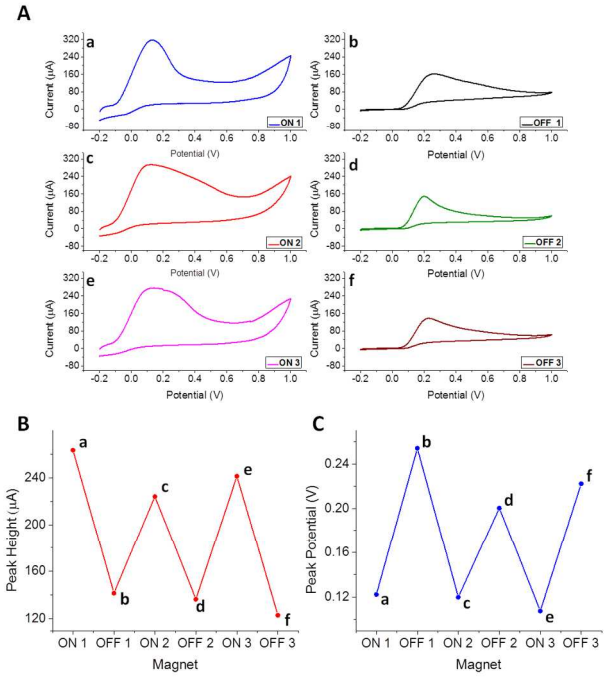

Figure 4. (A) Cyclic voltammograms of 10 mM ascorbic acid on Fe-TRGO with magnetic activation (a, c, e) and deactivation (b, d, f) of electrode for three cycles, and changes in (B) peak height and (C) peak potential during the cycles. Conditions: 50 mM PBS background electrolyte, scan rate 100 mV s^{-1}.

The electrocatalytic properties of the Fe-TRGO material for the oxidation of ascorbic acid were evaluated by monitoring the intensity of the signal as well as the oxidation potential. It can be seen in Figure 4A that larger oxidation peaks were observed when the magnetic graphene material was focused onto the working electrode using the magnet, while significantly smaller signals were observed upon deactivation. Peak heights of the oxidation signals were greatly enhanced, recorded at about 243 μA (Figure 4B, a, c, e) and dwindled to about 134 μA (Figure 4B, b, d, f) upon activation and deactivation, respectively. Similar results were obtained when the oxidation potentials were analysed as shown in Figure 4C. The peak potentials were 122, 254, 120, 200, 108 and 222 mV during the six switching steps, clearly indicating that an electrocatalytic process took place during the activation steps, as demonstrated by the lowering of the oxidation potential.

Reproducible switching was accomplished and no memory effect resulted since the cyclic placements and removals of the magnetic graphene did not result in major changes in the peak heights and peak potentials of the signals observed. Apart from the influence of the metal dopant, the enhanced sensitivity and lower peak potentials observed owe largely to the large surface area and strong electrocatalytic properties of the TRGO, which has been well-known for effective electrochemical sensing and other applications.[21]

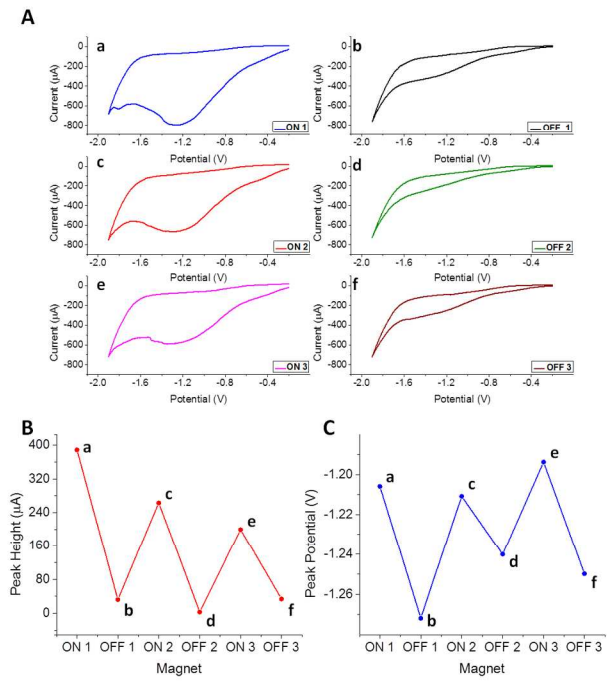

Figure 5. (A) Cyclic voltammograms of 10 mM cumene hydroperoxide on Fe-TRGO with magnetic activation (a, c, e) and deactivation (b, d, f) of electrode for three cycles, and changes in (B) peak height and (C) peak potential during the cycles. Conditions: 50 mM PBS background electrolyte, scan rate 100 mV s^{-1}.

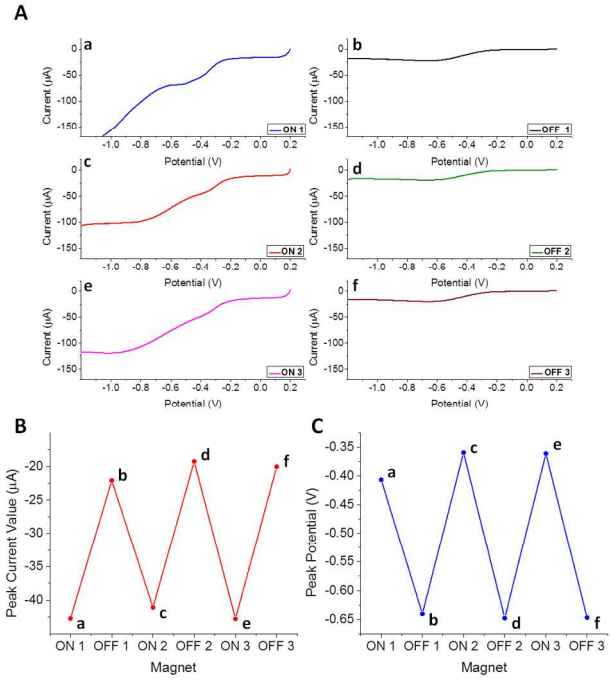

Figure 6. (A) Linear sweep voltammograms of 10 mM potassium hydroxide on Fe-TRGO with magnetic activation (a, c, e) and deactivation (b, d, f) of electrode for three cycles, and changes in (B) peak height and (C) peak potential during the cycles. Conditions: 50 mM PBS background electrolyte, scan rate 100 mV s^{-1}.

Electrocatalytic properties of Fe-TRGO were also studied for the possible catalytic effects of the Fe particles present which are recognized for catalysing the reduction of hydrogen peroxides,[22,23] other peroxides[19] and cumene hydroperoxide.[20, 24,25] Figure 5A displays the CV scans for the reduction of cumene hydroperoxide (CHP) with alternate attractions and removals of Fe-TRGO onto and off the working electrode surface. Apparent reduction peaks at around –1.20 V were observed when the electrochemical process was activated, while deactivated states yielded broad and barely visible peaks at approximately –1.25 V, as summarised in the peak potential comparison plot in Figure 5C. Figure 5B exemplifies that electrode surface sensitivity was largely enhanced upon attachment of the magnetic graphene materials. A significant difference in current signal was observed with values switching between 300 μA and 40 μA upon activation and deactivation, respectively.

Similar to previous findings, the controlled magnetic-switchable electrochemical process is repeatable from the study of CHP reduction. The peak heights and peak potentials remained larger and less negative, respectively, at activated states, and this distinct trend validates the feasibility in controlling reactivities of electrochemical processes with an external magnetic source.

Finally, the ability of the Fe-TRGO in inducing magnetically-switchable electrochemical reactivity was tested for the oxygen reduction reaction (ORR). Linear sweep voltammetry was used in this study (Figure 6A) to attain more discernible results, and it is apparent that clearer reduction signals were seen upon the activation while deactivation led to broad and flat responses. Peak current values were compared for the three repeated cycles at a fixed potential (around 350 mV), as summarized in Figure 6B. During activation, more negative peak current values were achieved, with a difference of about 20 μA between the activation and deactivation steps. Figure 6C illustrates the main peak potentials of the six switching steps, which were –406, –640, –359, –648, –361, –647 mV, from a to f, respectively. The significant difference of almost 300 mV between the activation and deactivation steps is a key indication of the outstanding catalytic properties of the Fe-TRGO.

High consistencies in the peak current values and peak potentials between the two modes were also evident, implying that electrode reactivity and responses of the reduction process were well-controlled by the external magnetic field with good repeatability. These observations coincide with the results from aforementioned studies, therefore proving the capability of switchable magnetically-controlled electrochemical processes.

Conclusions

On-demand control and selectivity has been a huge challenge for sensing & energy applications in the field of

electrochemistry. In this work, we presented a viable solution by proposing a magnetically-switching method which can control reversibly the electrochemical reactivity of a sensing system without much apparent carryover. An iron-doped thermally reduced graphene material have been synthesized and used as magnetic modifiers of a carbon based electrode. A permanent magnet underneath the electrode allowed easy control of the Fe-TRGO material which was positioned onto the working electrode surface (for the activated state or ON) or outside the working electrode surface (for the deactivated state or OFF). Significant differences in electrochemical properties resulted between the two states, with larger current signals recorded during the activation. Catalytic properties were also significantly different, as exhibited by evident potential shifts. In particular, lower potentials were recorded for the electrooxidation of ascorbic acid during the activation state. Not only did the high iron content introduce magnetic properties to the graphene material, it also acted as an efficient catalyst as established in the reduction of cumene hydroperoxide. The proposed methodology is highly scalable as it sheds light on possible adjustments on current sensing applications and prospective developments for future industrial purposes.

Acknowledgements

M.P. acknowledges Tier 2 grant (MOE2013-T2-1-056; ARC 35/13) from Ministry of Education, Singapore. Z.S. was supported by Specific university research (MSMT No. 20/2014).

Notes and references

a Division of Chemistry & Biological Chemistry, School of Physical and Mathematical Sciences, Nanyang Technological University, Singapore 637371, Singapore

b Department of Inorganic Chemistry, Institute of Chemical Technology, Technická 5, 166 28 Prague 6, Czech Republic

1 Geim, A. K.; Novoselov, K. S. *Nat. Mater.* 2007, **6**, 183.
2 Allen, M. J.; Tung, V. C.; Kaner, R. B. *Chem. Rev.* 2010, **110**, 132.
3 Novoselov, K. S.; Geim, A. K.; Morozov, S. V.; Jiang, D.; Zhang, Y.; Dubonos, S. V.; Grigorieva, I. V.; Firsov, A. A. *Science.* 2004, **306**, 666.
4 Pumera, M. *Chem. Rec.* 2012, **12**, 201.
5 Guo, B.; Fang, L.; Zhang, B.; Gong, J. R. *Insciences J.* 2011, **1**, 80.
6 Ambrosi, A.; Bonanni, A.; Sofer, Z.; Cross, J. S.; Pumera, M. *Chem. Eur. J.* 2011, **17**, 10763.
7 Gutes, A.; Hsia, B.; Sussman, A.; Mickelson, W.; Zettl, A. Carraro, C.; Maboudian, R. *Nanoscale.* 2012, **4**, 438.
8 Liu, X.-W.; Mao, J.-J.; Liu, P.-D.; Wei, X.-W. *Carbon.* 2011, **49**, 477.
9 Tang, Y.-B.; Yin, L.-C.; Yang, Y.; Bo, X.-H.; Cao, Y.-L.; Wang, H.-E.; Zhang, W.-J.; Bello, I.; Lee, S.-T.; Cheng H.-M.; Lee, C.-S. *ACS Nano.* 2012, **6**, 1970.
10 Endo, M.; Hayashi, T.; Hong, S.-H.; Enoki, T.; Dresselhaus, M. S. *J. Appl. Phys.* 2001, **90**, 5670.
11 Kamat, P. V. *J. Phys. Chem. Lett.* 2009, **1**, 520.
12 Musameh, M.; Wang, J. *Langmuir.* 2005, **21**, 8565.
13 Wang, J. *Electroanalysis.* 2008, **20**. 611.
14 Jin, G.-P.; Baron, R.; Rees, N. V.; Xiao, L.; Compton, R. G. *New J. Chem.* 2009, **33**, 107.
15 Wang, J.; Musameh, M.; Laocharoensuk, R. *Electrochem. Commun.* 2005, **7**, 652.
16 Hummers, W. S.; Offeman, R. E. *J. Am. Chem. Soc.* 1958, **80**, 1339.
17 Pumera, M.; Iwai, H. *J. Phys. Chem. C.* 2009, **113**, 4401.
18 Chua, C. K.; Sofer, Z.; Pumera, M. *Chem. Eur. J.* 2012, **18**, 13453.
19 Stuart, E. J. E.; Pumera, M. *J. Phys Chem. C* 2010, **114**, 21296.
20 Ambrosi, A.; Chua, C. K.; Khezri, B.; Sofer, Z.; Webster, R. D.; Pumera, M. *Proc. Natl. Acad. Sci.* 2012, **19**, 12899.
21 Pumera, M. *Materials Today.* 2011, **14**, 308.
22 Sljukic, B.; Banks, C. E.; Compton, R. G. *Nano. Lett.* 2006, **6**, 1556.
23 Gara, M.; Laborda, E.; Holdway, P.; Crossley, A.; Jones, C. J. V.; Compton, R. G. *Phys. Chem. Chem. Phys.* 2013, **15**, 19487.
24 Ambrosi, A.; Pumera, M. *Nanoscale.* 2014, **6**, 472.
25 Ambrosi, A.; Chee, S. Y.; Khezri, B.; Webster, R. D.; Sofer, Z.; Pumera, M. *Angew. Chem. Int. Ed.* 2012, **51**, 500.